Modulation of cortical slow oscillatory rhythm by $GABA_B$ receptors: an experimental and computational study

Perez-Zabalza M[1]*, Reig R[2]*, Manrique J[3]*, Jercog D[1], Winograd M[2], Parga N[3]‡ & Sanchez-Vives MV[4,5]‡

Modulation of cortical slow oscillatory rhythm by $GABA_B$ receptors: an experimental and computational study. BioRxiv

[1] Institut d'Investigaciones Biomediques August Pi i Sunyer (IDIBAPS), Barcelona, Spain

[2] Instituto de Neurociencias de Alicante, Alicante, Spain
[3] Física Teórica, Universidad Autónoma Madrid, Madrid, Spain
[4] ICREA, Barcelona, Spain

*equal contributions
‡ shared senior authorship

Current affiliation

Perez-Zabalza: Biomedical Signal Interpretation and Computational Simulation Group, University of Zaragoza, Spain

Jercog: Neurocentre Magendie - INSERM U 1215 - 146, rue Léo Saignat - 33077 Bordeaux

Keywords: Cerebral cortex/Up states/Inhibition/Computer model/Slow oscillations/Neocortical/Rhythms/Synchronization

Abstract

Slow wave oscillations (SWO) dominate cortical activity during deep sleep, anesthesia and in some brain lesions. SWO consist of Up states or periods of activity interspersed with Down states or periods of silence. The rhythmicity expressed during SWO integrates neuronal and connectivity properties of the network and it is often altered in neurological pathological conditions. Different mechanisms have been proposed to drive the transitions between Up and Down states, in particular, adaptation mechanisms have been proposed to contribute to the Up-to-Down transition. Synaptic inhibition, and specially $GABA_B$ receptors, have also been proposed to have a role in the termination of Up states. The interplay between these two potential mechanisms, adaptation and inhibition, is not well understood and the role of slow inhibition is not yet clear regarding the full cycle of the slow oscillatory rhythm. Here we contribute to its understanding by combining experimental and computational techniques. $GABA_B$ receptors-blockade not only elongated Up states, but also affected the subsequent Down states, and thus the whole cycle of the oscillations. Furthermore, while adaptation tends to yield a rather regular behavior, $GABA_B$ receptors-blockade decreased the variability of the sequence of Up and Down states. Interestingly, variability changes could be accomplished in two different ways: either accompanied by a shortening or by a lengthening of the duration of the Down state. Even when the most common observation is the lengthening of the Down states, both changes are expressed experimentally and also in numerical simulations. Our simulations suggest that the sluggishness of $GABA_B$ receptors to follow the excitatory fluctuations of the cortical network can explain these different network dynamics modulated by $GABA_B$ receptors.

Introduction

Different brain states are characterized by diverse patterns of spontaneous activity. The interplay between neuromodulators, receptors, intrinsic properties, and connectivity helps explain neuronal discharge, and as a network property, the emergence of different frequencies of oscillatory activity. During slow wave sleep, the synchronized discharge of a large number of cortical neurons explains the increase in voltage fluctuations observed during EEG recordings, whereas wakefulness and REM sleep can be identified by lower-voltage amplitudes (Aserinsky and Kleitman, 1953), reflecting a decrease in the number of cortical neurons discharging simultaneously. We also know that the degree of network synchronization/ desynchronization changes between different brain states and is precisely modulated during wakefulness as well (Poulet and Petersen, 2008; Okun et al., 2010; Harris and Thiele, 2011).

The modulation of network synchronization has been related to different brain functions. During slow wave oscillations (SWO) high levels of synchronization are involved in synaptic and cellular homeostasis, as well as memory formation (Hoffman et al., 2007; Diekelmann and Born, 2010; Tononi and Cirelli, 2014). It has been suggested that, during wakefulness, synchronization facilitates the transfer of information between distal neurons, providing temporal coordination for specific neuronal assemblies (Varela et al., 2001; Doesburg et al., 2010; Tononi and Cirelli, 2014). On the other hand, low levels of synchronization are observed during alert or attentional states, short-term memory tasks, or movements, at local cortical areas (Stancák and Pfurtscheller, 1996; Klimesch et al., 2007; Okun and Lampl, 2008; Doesburg et al., 2010). Malfunctions controlling neural synchronization at different oscillatory frequencies are related to several neurological diseases such as Alzheimer's (Busche et al., 2015; Castano-Prat et al., 2019), early aging (Castano-Prat et al., 2017), Parkinson's (Little and Brown, 2014), autism (Rubenstein and Merzenich, 2003), Williams Beuren syndrome (Dasilva et al., 2019), or Down Syndrome (Ruiz-Mejias et al., 2016), among others. Although the control of the degree of synchronization of neural activity is essential in order to understand normal and pathological brain function, there are still open questions regarding the basic mechanisms underlying network synchronization.

SWO (<1Hz) are organized into alternating periods of activity and silence–Up and Down states, respectively (Steriade et al., 1993). This spontaneous neural activity can be recorded from both isolated cortical slabs *in vivo* (Timofeev et al., 2000) and in cortical brain slices *in vitro* (Sanchez-Vives and McCormick, 2000) implying that the cortical network can generate SWO on their own (i.e., without external input). Indeed, SWO are also expressed in clinical conditions where a "cortical island" occurs as a result of a lesion (Gloor et al., 1977) or perilesional around acute ischemic cortical stroke, where SWO can persist for months or even years (Butz et al., 2004). This capability of the disconnected cortical network to generate highly similar SWO independently from the size of the cortex involved, has led to the suggestion that this SWO is the default emergent activity pattern from the cortical network (Sanchez-Vives and Mattia, 2014; Sanchez-Vives et al., 2017). Cortical SWO either in sleep or in deep anesthesia are characterized by a high degree of network synchronization, where large populations of neurons are engaged, shaping the slow wave sleep cycle (Bullock and McClune, 1989; Steriade et al., 1993; Destexhe et al., 1999; Ruiz-Mejias et al., 2011; Bettinardi et al., 2015). This synchronization can be explained by a combination of excitatory and inhibitory input that cortical neurons receive during Up states, which results in the depolarization of neuron membrane potential that, in turn, often generates bursts of action potentials. On the other hand, cortical activity during Down states remains rather silent. Such patterns of active and silent cortical activity depend on the balance between recurrent excitation and local inhibition (Sanchez-Vives and McCormick, 2000; Compte et al., 2003, 2009; Shu et al., 2003). However, the precise biophysical mechanisms underlying the inhibitory modulation of SWO is not fully understood.

In order to understand spontaneous SWO, several studies have proposed potential mechanisms responsible for their generation (transition from Down to Up states), maintenance, and termination (transition from Up to Down states). In terms of finalization, four main different mechanisms have been proposed that mediate the transition from Up to Down states: firing rate adaptation (Compte et al., 2003; Sanchez-Vives et al., 2010), short-term synaptic dynamics (Timofeev et al., 2000; Melamed et al., 2008; Benita et al., 2012), ATP-dependent homeostatic mechanisms

mediated by ATP-modulated potassium (K_{ATP}) channels (Cunningham et al., 2006), and pre- and post-synaptic $GABA_B$ (gamma-aminobutyric acid B) receptor activation (Parga and Abbott, 2007; Mann et al., 2009; Wang et al., 2010; Craig et al., 2013) (Sanchez-Vives et al., in review). It is plausible that more than one of these mechanisms interact and contribute to the termination of the Up-to-Down state transition; however, this is not yet well understood due to a paucity of experimental and modeling work addressing this issue. Although there are some indications that firing rate adaptation is at least partly responsible for the termination of Down states (i.e. generation of SWO) (Sanchez-Vives et al., 2010), it is not known to which extent this is the dominant mechanism. Interestingly, modeling work has shown that $GABA_B$ dynamics have the correct timescale to contribute to the Down state transition (Parga and Abbott, 2007) and that they could interact with firing rate adaptation to modulate the termination of Up states.

Here we combined biological and computational experiments to elucidate which mechanisms underlie modulation of SWO. More specifically, we empirically studied the role of $GABA_B$ receptors in controlling the Up to Down state transitions, Up and Down states durations and variability, and their impact on the global synchronization of spontaneous activity. We also modeled and simulated two different network behaviors and tested hypotheses in order to understand the role of each of the possible biophysical mechanisms in the modulation of SWO; finally, we tested the predictions obtained from the experimental observations in our models.

Methods

Experimental procedures

To empirically study the role of $GABA_B$ receptors in the modulation of SWO, *in vitro* experiments were performed on 37 ferret cortical slices (4- to 10-month-old, either sex). Ferrets were deeply anesthetized with sodium pentobarbital (40 mg/kg) and decapitated. Their brains were quickly removed and placed in ice-cold cutting solution (4–10°C). Coronal slices (thickness: 400 µm) of the primary visual cortex (n=24) and prefrontal cortex (n=13) were cut on a vibratome.

A modification of the sucrose-substitution technique developed by (Aghajanian and Rasmussen, 1989) was used to increase tissue viability, as in (Sanchez-Vives and McCormick, 2000). After preparation, slices were placed in an interface-style recording chamber (Fine Science Tools, Foster City, CA) and bathed in artificial cerebrospinal fluid (ACSF) containing (in mM): NaCl, 124; KCl, 2.5; $MgSO_4$, 2; $NaHPO_4$, 1.25; $CaCl_2$, 2; $NaHCO_3$, 26; and dextrose, 10; and was aerated with 95% O_2 and 5% CO_2 to a final pH of 7.4. Bath temperature was maintained at 34–35°C. After 2 h recovery, the ACSF was replaced by "*in vivo*-like" ACSF (Sanchez-Vives and McCormick, 2000) containing (in mM): KCl, 3.5; $MgSO_4$, 1; $CaCl_2$, 1; the remaining components were the same as those just described. Extracellular, unfiltered recordings were obtained by means of tungsten electrodes through a Neurolog system (Digitimer) amplifier. Intra and extracellular recordings were digitized, acquired using a data acquisition interface (CED) and software (Spike2) from Cambridge Electronic Design.

To study the effects of $GABA_B$ blockade on SWO, $GABA_B$ antagonist CGP 35348 (200µM) (Tocris) was added to the bath. Baseline recordings before CGP 35348 application were used as the control conditions.

In a subset of experiments (n=13), we recorded extracellularly from deep cortical layers before and after eliminating layer 1 from the cortical circuit. To isolate the circuit from long-lasting connections, a cut was made between layers 1 and 2/3, parallel to the white matter, and two additional cuts were made perpendicular to the

white matter (Fig. S1). To study $GABA_B$ blockade before and after isolating the circuit, $GABA_B$ blocker CGP 35348 (200μM) (Tocris) was added to the bath (n=11). Baseline recordings before cutting and before CGP 35348 application were used as the control conditions.

Spike recording and analysis

Extracellular multiunit recordings were obtained with 2–4 MΩ tungsten electrodes (FHC, Bowdoinham, ME). Multiunit activity (MUA) was estimated as the power change in the Fourier components at high frequencies of the recorded local field potentials (LFP). High-frequency components of LFP can be seen as a linear transform of the instantaneous firing rate of the neurons surrounding the electrode tip. We then assume that the normalized LFP spectra provides a good estimate of the population firing rate, given that Fourier components at high frequencies have power densities proportional to the spiking activity of the involved neurons.

Several parameters were quantified from the transformed signal (log(MUA)): (1) the maximum firing rate in the Up state was the peak of the average log(MUA) in the time interval (−0.5, 2.5 ms) around the Up state onset; (2) the upward and downward transition slopes were the gradients of the linear fits of the average log(MUA) in the time intervals (−10, 25 ms) and (−25, 10 ms), respectively, around the Up-state onset and offset, respectively; and (3) to measure the variability of SWO, we calculated the coefficients of variation (CV) (standard deviation/mean) of Up state duration, Down state duration and oscillation cycle duration (Up state duration + Down state duration). Data are reported as mean±SD. All off-line analyses were implemented in MATLAB (The MathWorks Inc., Natick, MA).

Model and theoretical procedures

To better understand the role of $GABA_B$ receptors in the modulation of SWO, we simulated networks of integrate-and-fire neurons, with the addition of a nonlinear membrane current, receiving synaptic input composed of slow and fast excitatory and inhibitory conductances (Parga and Abbott, 2007). These simulated networks consist of random connections with finite range. Each neuron is described by its membrane

potential V which, below its threshold value, evolves according to the equation

$$\tau_m \frac{dV}{dt} = -g_L(V - V_L) - g_a(V - V_a) - I_{syn,E} - I_{syn,I} - I_{noise} - I_{nl}. \qquad (1)$$

Here, τ_m is the membrane time constant, g_L is the leak conductance and V_L is the leak reversal potential. The adaptation current, g_a $(V - V_a)$, only affects the excitatory neurons. Its conductance, g_a, decays exponentially with a time constant, τ_a, until a spike is fired. When this happens, the adaptation conductance is augmented by an amount g_a. $I_{syn,E}$ and $I_{syn,I}$ are the excitatory and inhibitory synaptic currents, respectively. I_{noise} is an external noise current. I_{nl} describes a nonlinear property of the neuron (see below). A neuron fires whenever its membrane potential $V(t)$ reaches the spike generation threshold V_{th}. At this point, an action potential is triggered, and the potential $V(t)$ is reset and kept at a value V_{reset} during a refractory period τ_{ref}. Two excitatory (AMPA, NMDA) and two inhibitory ($GABA_A$, $GABA_B$) synaptic currents are included as $I_{syn,E}(t) = g_{AMPA}(V(t) - V_{AMPA}) + g_{NMDA}(V(t) - V_{NMDA})$

$$I_{syn,I}(t) = g_{GABAA}(V(t) - V_{GABAA}) + g_{GABA\,B}(V(t) - V_{GABA\,B}) .$$

When a neuron fires an action potential, the synaptic conductances of its postsynaptic neurons are modified by an amount Δg_X (X=AMPA, NMDA, and $GABA_A$, $GABA_B$). Otherwise, the synaptic conductances decay exponentially, with synaptic time constant τ_X. Nonlinearities characterizing NMDA and $GABA_B$ receptors are not considered; the emphasis in this model is on the time scales of the conductances. The nonlinear membrane current is a simple way of accounting for the neuron's intrinsic properties. It is described as

$$I_{nl}(t) = c\,(V(t) - V_1)(V(t) - V_2)(V(t) - V_3)$$

where $V_1 < V_2 < V_3$ and c determines the strength of the current. In the absence of noise, I_{nl} induces three fixed points, one of them being unstable. Fluctuations produced by the noise term and by the synaptic currents allow the neuron's membrane potential to alternate in a bistable fashion instead of being stuck at stable fixed-point values. Each neuron receives independent noise currents I_{noise} consisting of two filtered Poisson trains, one excitatory and one inhibitory. This current is

parameterized by two unitary conductances ($\Delta g_{syn,E}$ and $\Delta g_{syn,I}$), two Poisson rates and the time constants of the filter (τ_{NMDA} and τ_{GABAB}).

Parameter values

We simulated two networks (which we call the typical and atypical networks) in order to reproduce the experimentally observed data. These networks differ in parameters related to synaptic and adaptation properties (see below).

We also simulated networks with parameters as those of the typical network but with different values of the characteristic time of the adaptation current. Networks contained 4000 neurons of which 17% were inhibitory and the rest, excitatory. Pairs of neurons separated by a distance shorter than a certain radius were connected with a probability of 2%. This radius was chosen in such a way that, on average, each neuron was connected to 25 other neurons. The network size was 50 × 80 neurons, with periodic boundary conditions. All the neurons had a membrane time constant τ_m = 20 ms and a refractory time τ_{ref} = 5 ms. Other passive properties were distributed uniformly. The membrane threshold V_{th} took values of −45±2 mV, the reset potential V_{reset} of −55±1 mV, and the leak potential V_L of −68±1 mV. The parameters of the nonlinear current were c=0.03 mV^{-2}, V_1=−72±2 mV, V_2=−58±2 mV and V_3=−44±2 mV. AMPA and NMDA currents were present in all excitatory synapses. Similarly, we assigned $GABA_A$ receptors to 100% of the inhibitory synapses but $GABA_B$ receptors to only 70% of them.

The parameters of the noise model were: $\Delta g_{syn,E}$=0.09, $\Delta g_{syn,I}$=0.18 for the conductances and $\upsilon_{syn,E}$=66.66 Hz, $\upsilon_{syn,I}$=24.31 Hz for the frequency rates. The synaptic time constants were τ_{AMPA}=2 ms, τ_{NMDA}= 100 ms, τ_{GABAA} =10 ms, and τ_{GABAB}=200 ms. All conductances are measured in units of the excitatory leak conductance (which we took as $g_{E,L}$=10 nS). $\Delta g_{E,AMPA}$=0.54, $\Delta g_{E,NMDA}$=0.04, $\Delta g_{E,GABAA}$=1.00, $\Delta g_{E,GABAB}$=0.18. For inhibitory neurons, $\Delta g_{I,AMPA}$=0.38 (typical network) or $\Delta g_{I,AMPA}$=0.57 (atypical network), $\Delta g_{I,NMDA}$=0.04, $\Delta g_{I,GABAA}$=0.02, $\Delta g_{I,GABAB}$=0.017 and $g_{I,L}$=1.4. In addition, for excitatory neurons, Δg_a=0.03, V_a=−80 mV and τ_a= 1900 ms (typical network) or τ_a=2500 ms (atypical network). The

reversal potentials for the inhibition, V_{GABAB} and V_{GABAA} fall uniformly within the values −90±2 mV and −80±2 mV, respectively. V_{AMPA} and V_{NMDA} are both set to zero. We also considered another example of typical network with the same parameters as the one described above except for $\Delta g_{E,NMDA}$=0.05 , $\Delta g_{I,NMDA}$ =0.05 and τ_a= 4000 ms.

Up and Down transition detection algorithm

This algorithm provided criteria for determining when the network moved from one state to another. The criteria can be summarized as follows: (1) Up-to-Down transitions: at a given time, the number of spikes of each neuron in a window of 60 ms was measured. If every cell fired less than two spikes, the transition to the Down state took place. (2) Down-to-Up transitions: if the percentage of neurons that fired in windows of 60 and 100 ms was at least 10% and 30%, respectively, then the transition to the Up state occurred (Luczak et al., 2007).

Correlation functions and coefficients of variation (CV)

We calculated spike correlograms as the average over a subpopulation of 200 randomly selected neurons of the pair-wise correlation function

$$C(i,j,\tau) = \frac{\int \rho_i(t)\rho_j(t-\tau)dt}{r_i r_j}, \quad (2)$$

where $\rho_{i(j)}(t)$ and $r_{i(j)}$ are the spike train and the firing rate, respectively, of neuron i (j), and τ is the time lag. Correlation functions of the currents were computed as:

$$C\left(\tilde{I}_\alpha, \tilde{I}_\beta, \tau\right) = \int \tilde{I}_\alpha(t)\tilde{I}_\beta(t-\tau)dt \quad (3)$$

where $\tilde{I}_{\alpha(\beta)}$ is the population average of the current $I_{\alpha(\beta)}$. Both $C(i,j,\tau)$ and $C(\tilde{I}_\alpha, \tilde{I}_\beta, \tau)$ were normalized to their value at their respective peaks. CVs of the duration of the Up states, the Down states and the cycle were defined as the ratio between the standard deviation and the mean (standard deviation/mean).

Simulation

Simulation times were typically 1200 s. Differential equations were integrated using the Euler method with an integration step of Δt=0.1 ms. To obtain Fig. 7A, we ran eight simulations of 150 s for each value of the parameter τ_a, with different realizations of the noise. Statistical errors in these graphs were computed as the SD of the values obtained in each simulation. All codes were written in C and run under the Linux operating system.

Results

The cortical network *in vitro* preserves the mechanisms to generate spontaneous rhythmic neural activity, namely SWO, organized into Up states (active periods), and Down states (silent periods). Recordings from ferret cortical slices revealed spontaneous SWO (Fig. 1A).

Effects of $GABA_B$ blockade on the Up / Down state cycles

The baseline frequency of the slow oscillations was 0.35 ± 0.02 Hz, with a duration of Up/Down states of 0.56 ± 0.05 s and 2.55 ± 0.17 s respectively. $GABA_B$ antagonist CGP35348 applied to the bath resulted in the gradual blockade of slow inhibition and induced several changes in the Up and Down states of the cortical slices (n=37) (see Fig. 1 for a particular slice). In agreement with previous studies (Mann et al., 2009), a prominent and consistent change in Up and Down state properties upon $GABA_B$ blockade was the elongation of the Up states (Fig. 1A-F).

The Up state elongation resulting from $GABA_B$ blockade was observed in 34 out of the 37 slices (Fig. 1D, 1E, Fig. 2A and 3D, 3E), while there were no changes in the remaining three cases. This elongation was on average to 182% the original Up state duration and was observed independently of the original duration in the control (baseline) condition, which ranged between 0.2 and 1.3 seconds (Fig. 2A). The elongation of Up states following $GABA_B$ receptor blockade suggests that these receptors participate in the termination of the Up states, as it has been previously proposed (Parga and Abbott, 2007; Mann et al., 2009; Wang et al., 2010; Craig et al., 2013), although it could also be secondary to the alteration of the excitatory/inhibitory balance during the Up state and subsequent modulation of the firing rate during Up states (Compte et al., 2003; Mattia and Sanchez-Vives, 2012). We explore these possibilities next.

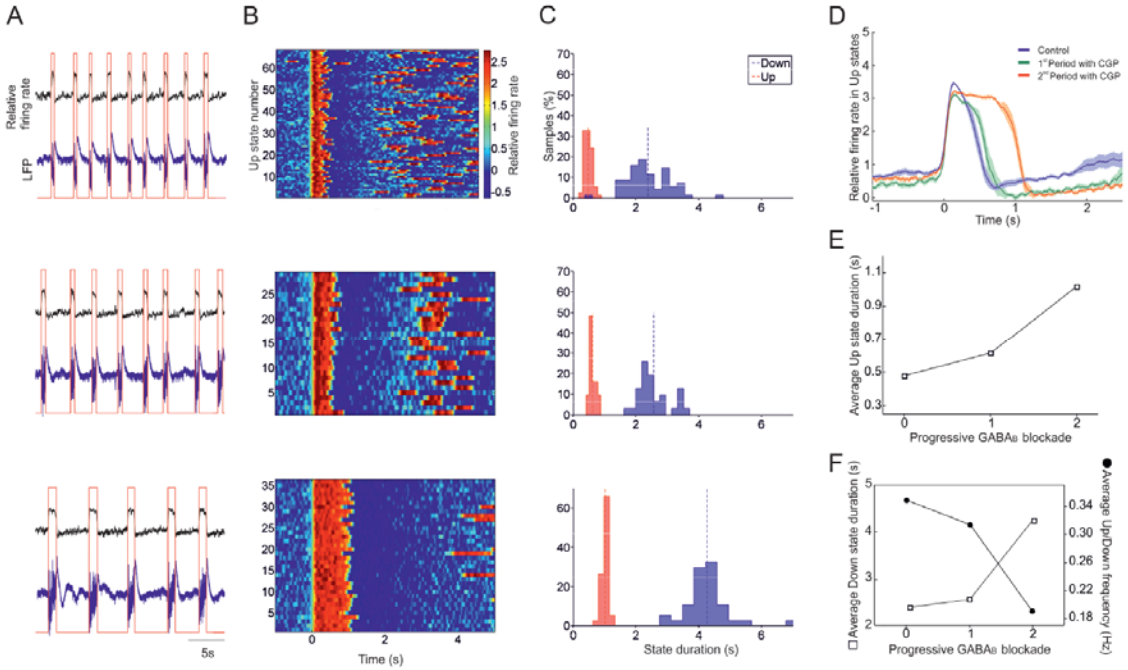

Figure 1. Effects of progressive inhibition blockade on slow oscillations. Typical network. A. Raw signal (blue trace) and relative firing rate (black trace; see Methods). Up states were detected from the relative firing rate (red trace). From top to bottom: control activity and two consecutive periods after application of 200 μM CGP 35348. Time scale is the same for all panels in A. **B.** Raster plots of the relative firing rate are represented for control activity and for 200 μM CGP 35348 corresponding to the ones in A. The firing rate is color coded. Time scale is the same for all panels in B. **C.** Histograms of the Up and Down duration for control activity and 200 μM CGP 35348 corresponding to the ones in A. **D.** Average relative firing rate for Up states during the control and 200 μM CGP 35348 corresponding to the ones in A. The shadow corresponds to the s.e.m. **E.** Up state duration increases with CGP 35348. **F.** Down state duration increases whereas the oscillation frequency decreases. Empty squares are average Down state duration and filled circles are average Up/Down frequency.

Down states were also globally elongated as a result of $GABA_B$ blockade. The average elongation of the Down state (n=37) was to the 138% of the original value (Fig. 1, Fig. 2). However, when recordings were looked at individually, we observed two patterns (or groups): even though the most common effect was the elongation of the Down states (n=28, Fig. 1; Fig. 2B), in some cases Down states were indeed shortened by $GABA_B$ blockade with CGP35348 (n=9, Fig. 2B; Fig. 3). We called the first group "typical" (Fig. 1) and the second one "atypical" (Fig. 3), and this is how we will refer to them in the rest of the study. The shortening of Down states could occur even when the Up states were elongated similarly to the typical case in Fig. 1, resulting in the overall increase of the frequency of the oscillatory cycle (Fig. 3F).

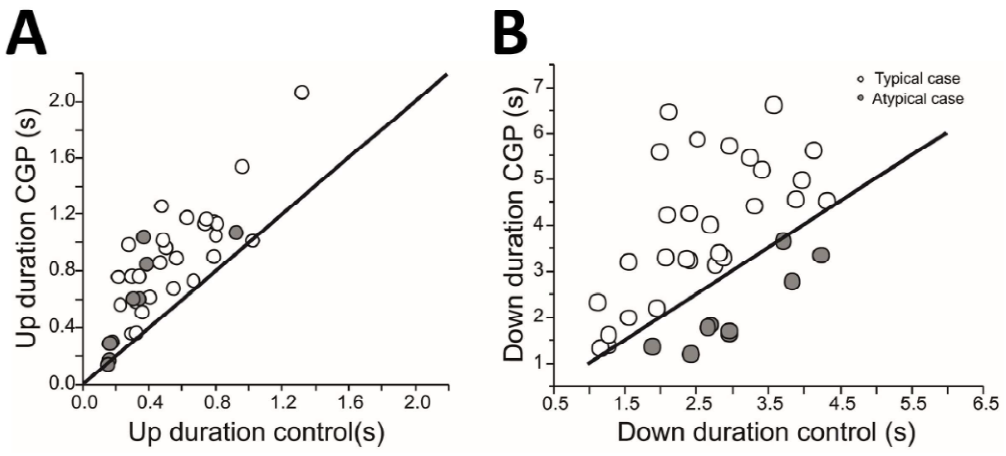

Figure 2. Modulation of Up and Down states by $GABA_B$-receptors. A, scatter plot of the duration of Up states in control *versus* blockade of $GABA_B$ receptors with 200 μM CGP 35348. In all cases the Up states duration increases or in few cases remains the same. **B**, same for Down state duration. In the two panels, the imaginary line is the one corresponding to the absence of changes (bisecting line). We define as "typical networks" those were the Down state duration gets elongated (empty circles), and "atypical networks" those in which the Down states got shorter (gray-filled circles).

Up and Down states are dynamically related (Compte et al., 2003; Sanchez-Vives et al., 2010; Mattia and Sanchez-Vives, 2012); it is therefore intriguing that the same transformation of the Up states (elongation) is followed by two different transformations of the Down states (typical elongation, or atypical shortening) (Fig. 2A, B). A possible functional explanation of these results could be that SWO in typical and atypical networks were different to start with. Indeed, we found that in control conditions, the Up state duration was significantly shorter in atypical than in typical networks (atypical: 0.32±0.08 s; typical: 0.56±0.05 s; $p<0.05$), although this observation still lacks a mechanistic explanation. We further explore the possible dynamical mechanisms in our computer model below.

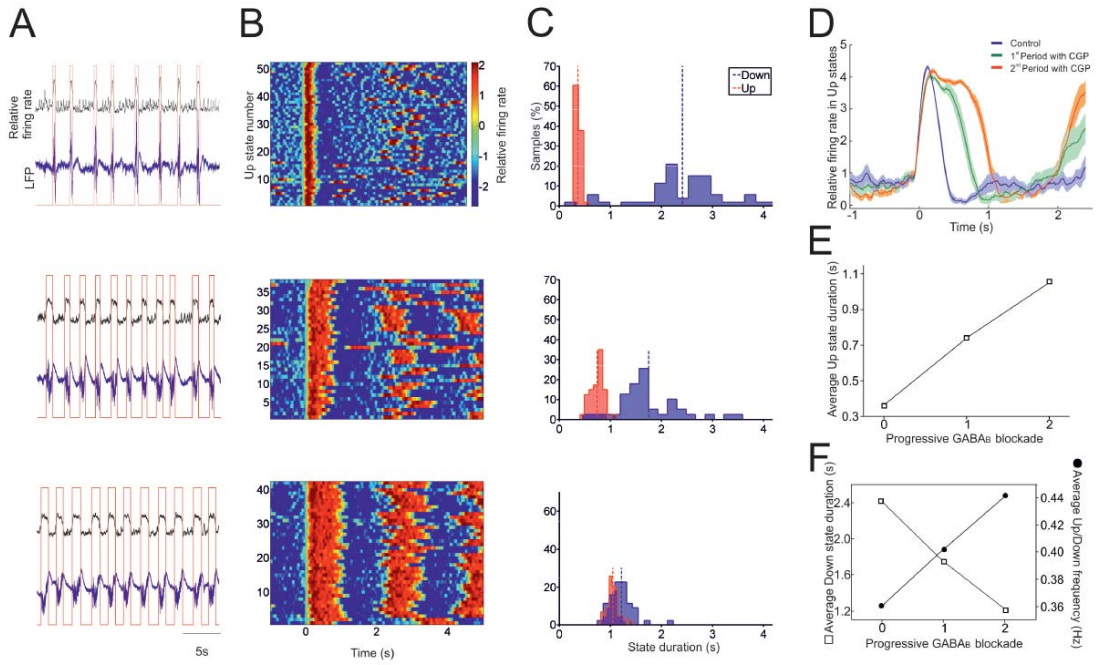

Figure 3. Effects of progressive inhibition blockade on slow oscillations. Atypical network. A. Raw signal (blue trace), relative firing rate (black trace; see Methods) and detected Up and Down states (red trace). From top to bottom: control activity and two consecutive periods after application of 200 μM CGP 35348. **B.** Raster plots of the relative firing rate are represented for control activity and for 200 μM CGP 35348 corresponding to the ones in A. The firing rate is color coded. **C.** Histograms of the Up and Down duration for control activity and 200 μM CGP 35348 corresponding to the ones in A. **D.** Average relative firing rate for Up states during the control and 200 μM CGP 35348 corresponding to the ones in A. The shadow corresponds to the s.e.m. **E.** Up state duration increases with CGP. **F.** Down state duration decreases whereas the oscillation frequency increases.

Interestingly, $GABA_B$ receptor blockade strikingly increased the regularity of the SWO. This effect was obvious in the autocorrelations of the activity before and after $GABA_B$ blockade, where the time constant of an exponential fitted to the peaks (coherence time (Dowse, 2009) became slower under $GABA_B$ blockade (Fig. 4A,B, insets in (a)).

The change in variability of the durations of Up and Down states and oscillatory cycles was also quantified by the coefficient of variation (CV). The CV of Up states in atypical networks, and also the CV of Down states and of the oscillatory cycle, were significantly decreased by $GABA_B$ blockade in both typical (Fig. 4Ad) and atypical (Fig. 4Bd) networks. Compared with control values, the decrease of the CV for the

typical case was to 85% and 68% for the Up and Down states, respectively, and to 66% for the complete oscillatory cycle (Fig. 5).

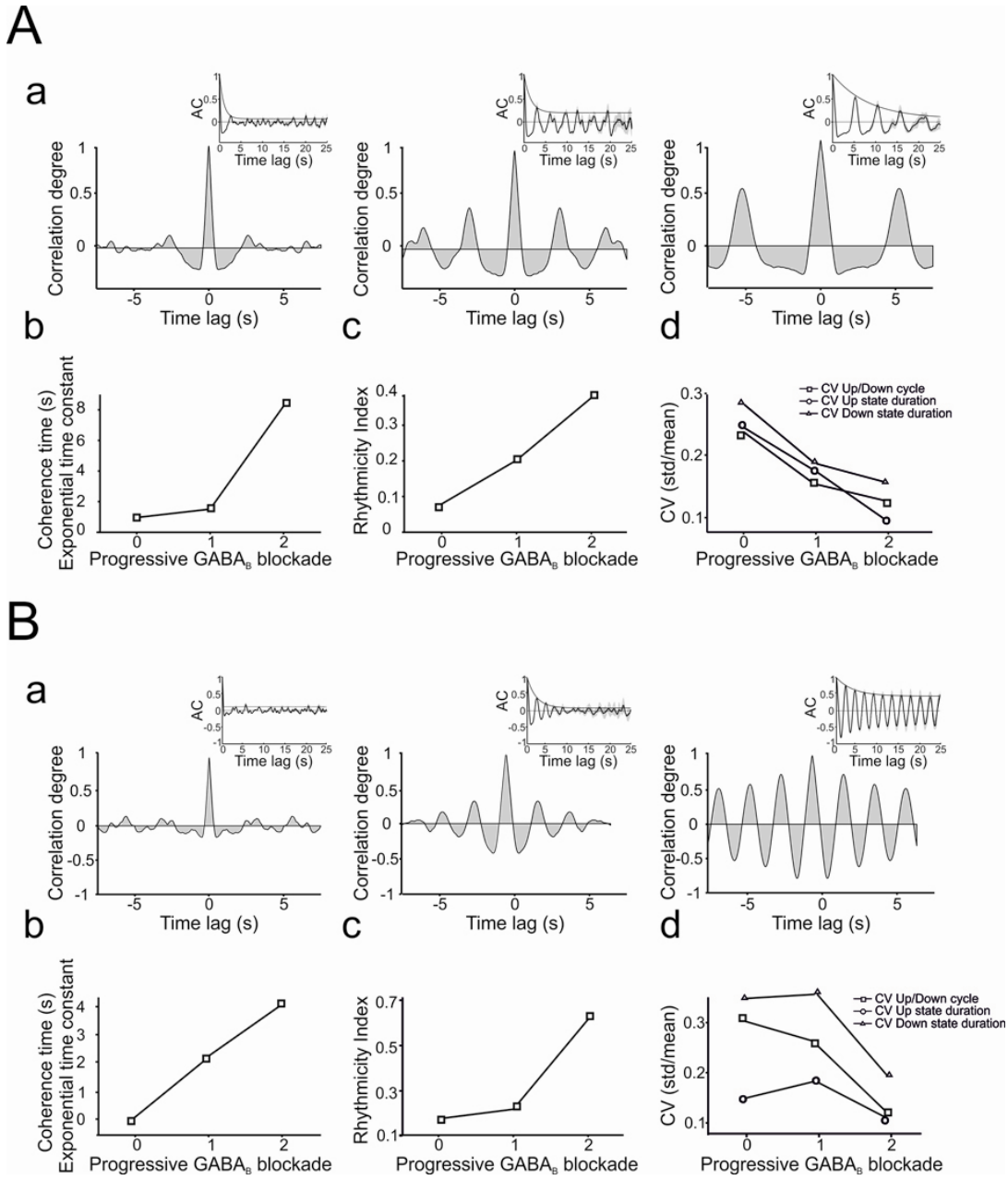

Figure 4. Effect of GABA$_B$ blockade on the variability of slow oscillations. A. 'Typical' network (same recording as Fig. 1). (a) Autocorrelograms illustrating the transformation of the emerging activity for control activity and for two consecutive periods after application 200 μM CGP35348 (left to right). Inset: The decay envelope of the autocorrelogram is a function of the long-range regularity in the signal (Chatfield, 1980). (b) Measure of the decay envelope of the autocorrelogram. (c) Rhythmicity Index. (d) CV of Up/Down cycle, Up state duration and Down state duration. **B.** 'Atypical' network (same recording as Fig.2). Same parameters that (A).

In the case of the atypical case there was a significant decrease in CV of 58% for the Down state, and 51% for the oscillatory cycle. These results indicate that the physiological activation of $GABA_B$ receptors introduces variability and dynamical richness in the spontaneous SWO. Hence, activation of $GABA_B$ receptors does not only contribute to the modulation of the duration of the Up states, but also affects the network dynamics by controlling the duration of the Up/Down states and by disrupting the regularity of the SWO (Fig. 5).

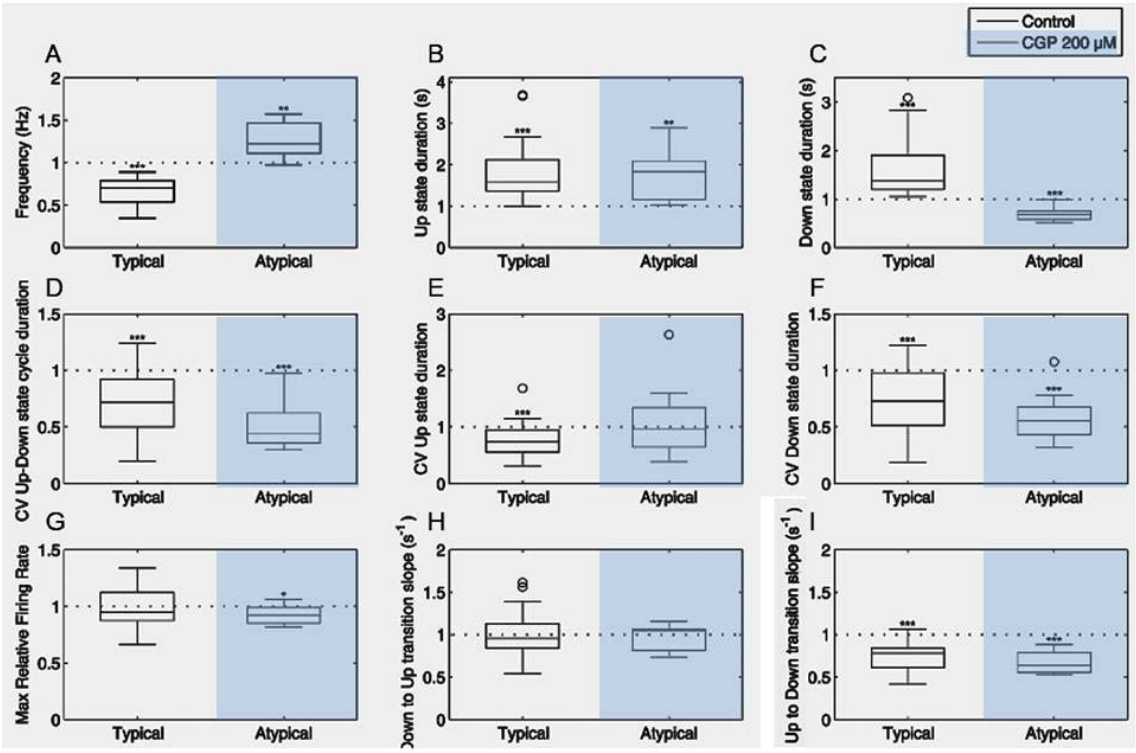

Figure 5. Relative changes of Up and Down states properties after removal of slow synaptic inhibition on typical (n=28) and atypical (n=9) network. Average values of different parameters calculated. A Student's t-test was used to evaluate how different the normalized averages were from 1.0., $p < 0.05$ (*); $p < 0.01$ (**); $p < 0.001$ (***).

The firing rate during Up states is in some cases the link that explains the Up/Down

state relative durations. This can be the case when the mechanisms of termination of Up states are activity-dependent, for example the activation of sodium- and calcium-dependent K^+ currents (Compte et al., 2003). In cases where $GABA_A$ receptors are blocked, the decrease in fast inhibition results in high firing rates during Up states that efficiently activate sodium- and calcium-dependent K^+ currents that shorten the Up states and elongate Down states (Sanchez-Vives et al., 2010). We explored if this was the case when $GABA_B$, and not $GABA_A$, receptors were blocked. We did not find any significant difference when comparing the firing rate in Up states before and after $GABA_B$ blockade (Fig. 5G; n=37). This finding suggests that the GABAergic control of firing rate in Up states mostly occurs through $GABA_A$ receptors, while the role of $GABA_B$ receptors on firing rate is negligible but noticeable on the termination of Up states and on network dynamics.

To understand the dynamics of the oscillatory activity in the cortical network is useful looking into the transitions between states, such as the slopes of the Down-to-Up and Up-to-Down transitions. The Down-to-Up transition slope, which corresponds to the recruitment of the local network (Reig et al., 2010; Sanchez-Vives et al., 2010) was not affected by $GABA_B$ receptor blockade. Interestingly, the Up-to-Down (downward) transition slope was significantly decreased (Fig. 5I) both in typical and atypical networks, meaning that the finalization of the SWO cycle was slower when $GABA_B$ receptors were blocked, further supporting the role of these receptors in the termination of Up states.

We investigated the possible role of cortical layer I in modulating the spontaneous Up and Down states in infragranular layers before and after $GABA_B$ blockade. To this end, we recorded spontaneous SWO before and after eliminating layer 1 from the cortical network by cutting the slice between layers 1 and 2/3, with and without $GABA_B$ blockade with CGP 35348 (Fig. S1A, n=11). $GABA_B$ blockade resulted in a significant elongation of the Up states even in the absence of layer 1, similar to what occurred in control slices (Up state duration: control 0.47±0.05 s; layer 1 eliminated 0.34±0.04; layer 1 eliminated + CGP 35348 0.53±0.04, Fig. S1). This result parallels a previous study showing that, during spontaneous oscillatory activity, $GABA_B$ contributes to the Up-to-Down state transitions without the influence of layer 1

(Craig et al., 2013).

In our study we also explored whether different circuits can display diverse effects after blocking $GABA_B$ receptors. For this, we recorded the spontaneous SWO in supra- and infragranular layers simultaneously with and without CGP 35348. The results did not show differences between layers (n=16). The effects on supragranular layers were not different to the ones described for infragranular layers in Figs 1 and 2. These results show that $GABA_B$ receptors strongly modulate the spontaneous neural activity in different layers and cortical areas as reported above.

In conclusion, from the experimental results we observed that the blockade of $GABA_B$ receptors decreased the variability (CV) of the duration of Up and Down states as well as of the complete oscillatory cycle, suggesting that $GABA_B$ receptor activation plays a key role desynchronizing network activity. We also observed a prominent and consistent elongation of Up states as a consequence of $GABA_B$ receptor blockade, confirming that $GABA_B$ activation participates on the termination of Up states. The fact that the slope of the Up-to-Down state transition became slower when $GABA_B$ receptors were blocked is in agreement with the suggested role of these receptors in Up state termination proposed by (Mann et al., 2009). In most cases the Up state elongation after $GABA_B$ blockade occurred concurrently with an elongation of the subsequent Down states (typical network), although in one-quarter of the cases the Down states shortened (atypical network). We designed a computer model of the cortical network that reproduces these observations and proposes a mechanistic explanation for them, proposing a role for $GABA_B$ receptors in the dynamics of the SWO.

The model: description of its basic properties

First, we present the basic features of the SWO generated with our model. We generated two sample networks, one responding to $GABA_B$ receptor blockade in a typical and the other in an atypical way. We next explored the most remarkable effects of $GABA_B$ receptors that were reported experimentally: modulation of the duration of the Up states and modulation of the regularity of the oscillations.

We generated several sample networks with fixed connectivity but differing in the precise realization of the connectivity matrix and in the value of some parameters (see Methods for details). Two examples of networks (typical and atypical) were defined such that they had approximately the same cycle duration in the control condition (Fig. 6A and 6B). For both networks, in all the generated samples and in all the slices recorded in our experiments, blocking $GABA_B$ receptors did not suppress the SWO, and the duration of the Up state became longer. For the typical network (Fig. 6A), the duration of the Down states increased as it did in the typical experimental cases. For the atypical network (Fig. 6B), the duration of the Down states decreased as it occurred in the atypical experimental cases as well. Notice that for the two networks, the histogram of the duration of Down states (panels b and e in Figs. 6A and 6B) had a larger dispersion when $GABA_B$ receptors were not blocked (control). To quantify the variability of the cycle and of the durations of the Up and Down states, we calculated their CV in the network. For the two networks (Fig. 6), the CV values were (typical (atypical)): 0.29 (0.34), 0.22 (0.25) and 0.20 (0.25) for the Down state, the Up state and the whole cycle duration, respectively, in the control condition; and 0.15 (0.15), 0.10 (0.20) and 0.13 (0.15) when $GABA_B$ receptors were blocked. These values showed a substantial decrease in variability following $GABA_B$ receptor blockade in both networks, especially for the duration of the Down states. Panels c and f in Figs. 6A and 6B illustrate the correlograms of the spike trains for the control and the $GABA_B$blocked conditions.

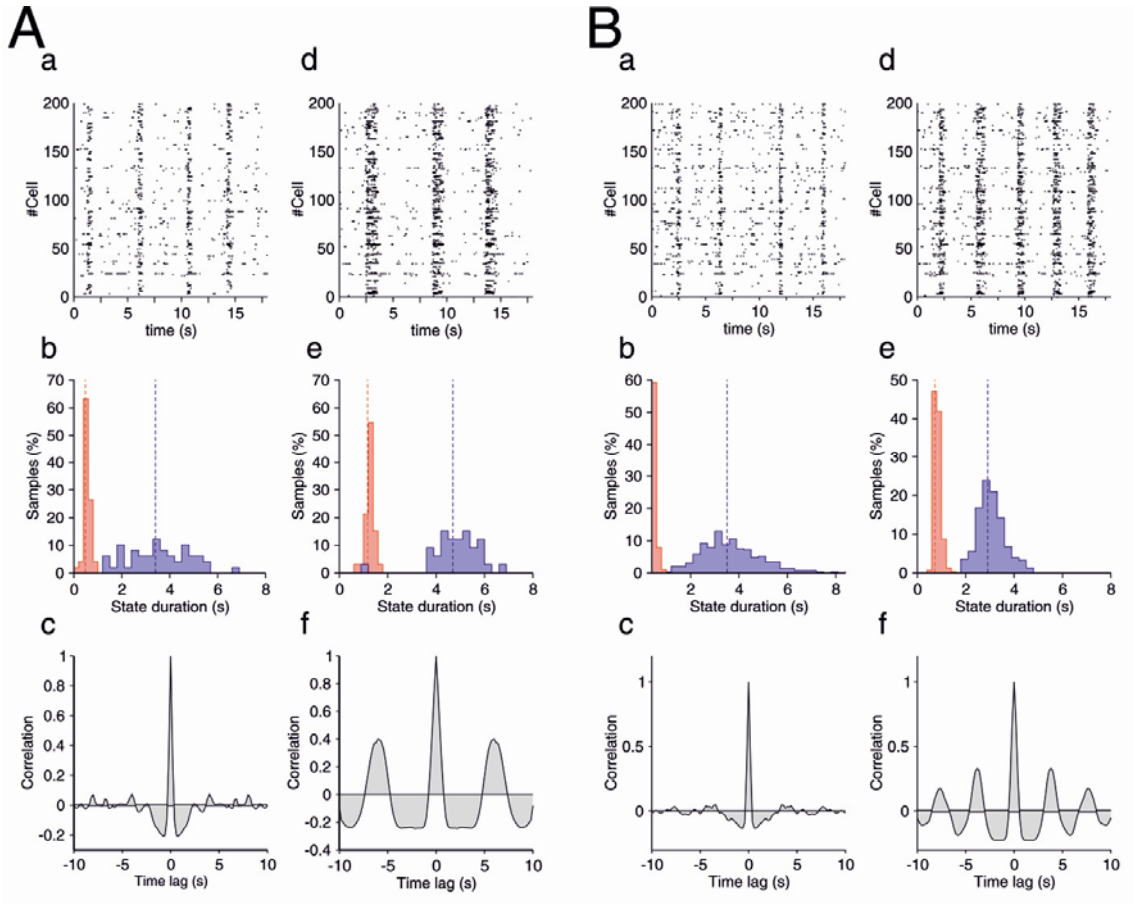

Figure 6A. Properties of the slow oscillation in a typical (A) and atypical (B) networks. A. Plots on the left refer to the control condition and on the right to the slice with blocked $GABA_B$ receptors. (a, d) Rastergrams. (b, e) Histograms of the duration of the Up (red) and Down (blue) states. Dashed lines correspond to their mean value: Mean durations of Up (Down) states are 0.45s (3.42s) in (b) and 1.17s (4.69s) in (e). (c, f) Spike-train correlation functions averaged over 100 pairs of neurons. Note how the oscillation becomes more regular in the blocked condition. **B.** Properties of the slow oscillation in an atypical network. Conventions are as in Figure 6A. Mean durations of Up (Down) states are 0.36s (3.51s) in (b) and 0.73s (2.91s) in (e).

Explaining the modulation of variability by $GABA_B$ receptors

In our experimental results we found that the decrease in the variability of the duration of Down states and complete cycles occurred in all cases, while the decrease in Up state duration variability only occurred in typical networks. To investigate the factors responsible for the variability of the Down state duration in our model, we looked at the traces of the synaptic and adaptation currents (Fig. 7A) for the two networks described in Fig 6.

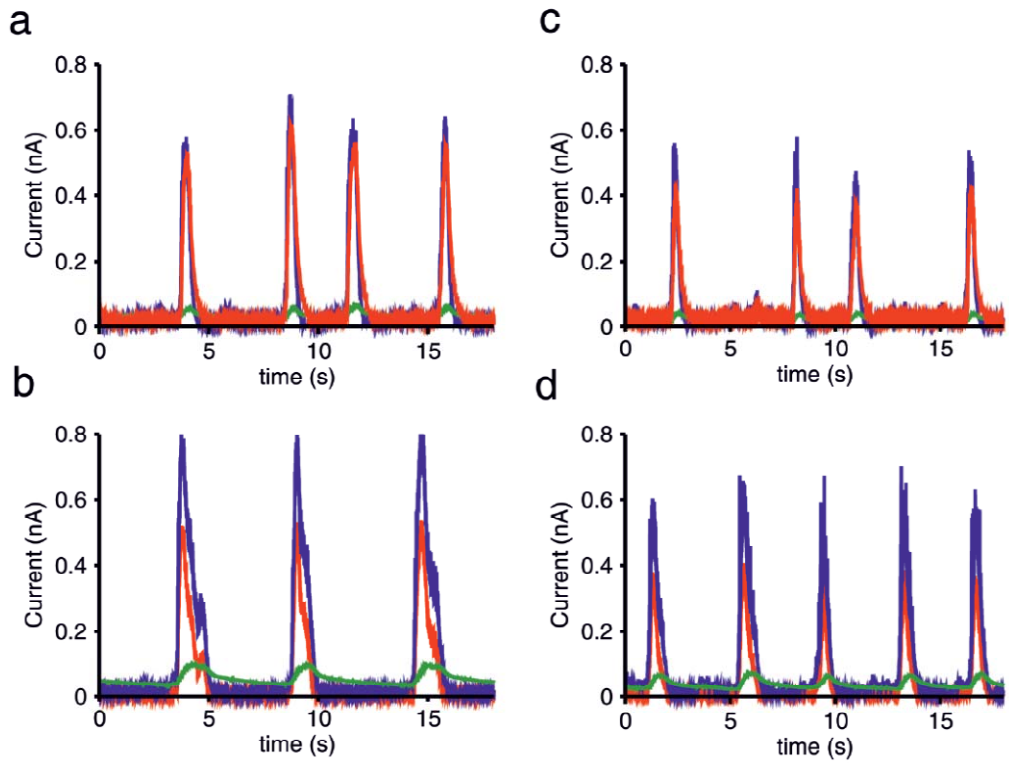

Figure 7. Temporal traces of the synaptic and adaptation currents. Temporal traces of the population averaged currents for the typical (left side) and the atypical (right side) network . Panels (a) and (c) refer to the control networks and panels (b) and (d) to the networks with the $GABA_B$ receptors blocked. Notice the increasing regularity in the blocked case. Blue lines: total excitatory (AMPA plus NMDA) current. Red lines: total inhibitory ($GABA_A$ plus $GABA_B$) current. Green lines: adaptation current.

We first examined why SWO were rather regular when $GABA_B$ receptors were blocked. Fluctuations of the neuronal excitation occur either from synaptic or external noise. Since in the $GABA_B$-blocked condition the inhibition is fast ($GABA_A$-mediated), fast inhibition can track these fluctuations easily (Compte et al., 2009; Renart et al., 2010) so that they do not propagate through the network unless a large population of excitatory neurons becomes active. Thus, the dynamics consist in a gradual increase of the excitation that starts during the Down state and grows until an Up state is generated (Fig. 7b and 7d). At this point the fast inhibition follows this large change in the excitation but cannot suppress it. During Up states, the

adaptation current progressively increases and produces the end of the Up state. Since the characteristic time of the adaptation conductance is large and spiking is rare during the Down state, this conductance decays smoothly and slowly. These mechanisms give rise to a rather regular sequence of cycles (Fig. 7A).

When $GABA_B$ receptors are not blocked, as in the case of the experimental control condition, these receptors produce two main effects. First, the total inhibitory current increases. A consequence of this increase is the shortening of the duration of the Up states (Fig. 6Aa,Ba and Fig. 7a,c). The second effect is the loss of regularity. Our experimental observations showed that when $GABA_B$ receptors were not blocked, Down states could either be longer or shorter than in the blocked condition, the second case being the most typical. In both, the typical (Fig. 6A) and the atypical (Fig. 6B) simulated networks, the variability was higher in the control condition, but the origin of this variability has to be explained differently because the mean duration of their Down states was related differently to the corresponding networks with blocked $GABA_B$ receptors.

For the atypical network (Fig. 6B), comparison of the temporal traces of the currents for the control and the blocked $GABA_B$ networks obtained with simulations (Fig.7Ac and Ad) indicate that some Up states were suppressed in the control condition. This increased the mean duration of the Down states (Fig. 6B) and increased their variability (from CV=0.15 to 0.34). For the typical network (Fig. 6A) the temporal traces of the currents (Fig. 7a and b) indicate that, in contrast to what happened for the atypical case, now new Up states appeared with respect to the blocked condition. This also introduced a similar change in the variability of the duration of the Down states (CV increased from 0.15 to 0.29). To explain this different behavior in typical vs. atypical networks, let us focus on the way that the two networks were constructed. These two networks differ in the value of only two parameters: the NMDA conductance and the characteristic time of the adaptation conductance.

In the typical network, the NMDA unitary conductance is 40% larger than in the atypical one. To see the effect of a larger NMDA conductance on the duration of the Down states, let us consider a network identical to the atypical one (Fig. 6B) but with

the NMDA unitary conductance increased by 40%. The stronger excitatory recurrent inputs reduced the duration of Down states in both, the control (Fig. 8A) and the blocked $GABA_B$ (Fig. 8B) conditions. This effect can be observed by comparing the mean duration of Down states for the modified network with the corresponding mean duration for the original atypical network (Fig. 8A and B). However, one important difference arises: in the control condition, the shortening of the duration of the Down states is about 68% while in the blocked $GABA_B$ condition it is only about 33%. Notice that this difference makes the original atypical network (Fig. 6B) become typical, in the sense that now the duration of Down states is longer when $GABA_B$ receptors are blocked.

Why this differential shortening of Down states? The explanation can be found in the cross-correlation function between the excitatory and inhibitory currents in the atypical network (Fig. 8C). In the blocked $GABA_B$ condition, the tracking of excitatory currents by inhibitory ones is almost instantaneous (the peak is located at 1.0 ms). A consequence of this is that inhibitory inputs can follow excitatory ones, until they are strong enough to cause the network to arrive to an Up state. However, in the control condition, the slow dynamics of the $GABA_B$ receptors make the tracking of the excitation by inhibition difficult. This fact is reflected in the peak of the cross-correlation function at 46.0 ms (Fig. 8C, full line). This lag is 86.0 ms if only the $GABA_B$ component of the inhibition is considered (dashed-dotted line). Since the tracking mechanism is not efficient in the control condition, the shortening of Down state duration is much more pronounced than in the blocked $GABA_B$ condition.

The two differences between these two sample simulated networks were NMDA conductance, which we have already described, and the time of the adaptation conductance. Both networks (Fig. 6) were selected such that they had approximately the same Down state duration in the control condition. Although the network in Fig. 8A,B is already a typical network, the mean duration of its Down states in the control condition is shorter than that of the atypical network in Fig. 6B. To obtain the typical network in Fig 6A, we then made the characteristic time of the adaptation conductance 50% larger than in the atypical network.

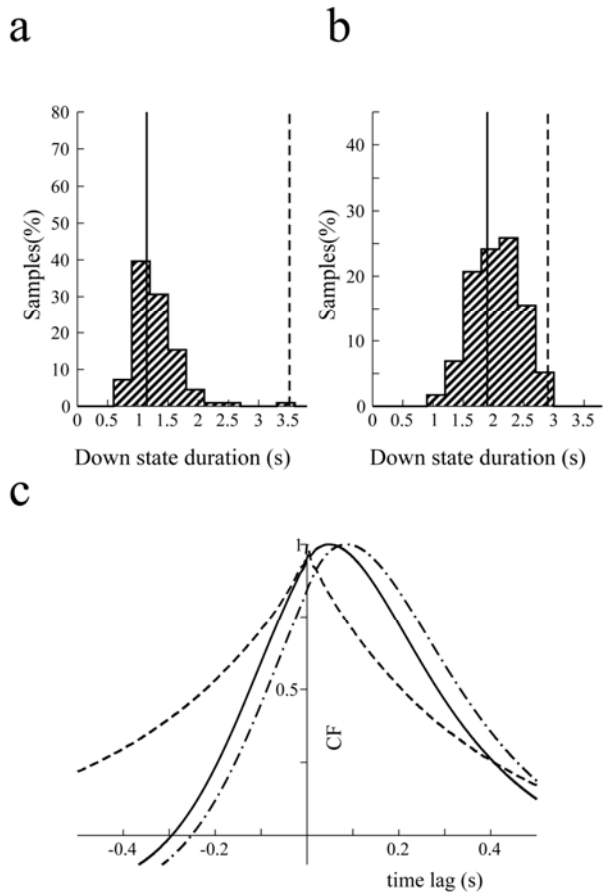

Figure 8. Effect of NMDA conductances on the duration of Down states. (a) Histograms of the duration of the Down states in the control condition of a network with the same parameters as the atypical one (Fig. 6B) but with NMDA unitary conductances increased 40%. Average Down state duration (solid line) is 1.1s, 68% smaller than in the original network, 3.51s (dashed line). (b) Same as (a) but in the blocked condition. Average Down states duration (solid line): 1.8s, about 33% smaller than in the original network, 2.91s (dashed line). (c) Correlation function between excitatory and inhibitory currents in the atypical network. Full line: Correlation function between total excitatory and inhibitory currents in the control condition. Dashed line: same as before but in the $GABA_B$ blocked condition. Dashed-dotted line: Correlation function between total excitation and $GABA_B$ component of the inhibition. CF, correlation function.

In conclusion, the tracking of fast inhibitory currents to the excitation in cortical networks (Compte et al., 2009; Renart et al., 2010) is therefore spoiled by the presence of $GABA_B$ currents spoiled this property.

Discussion

In this paper we investigated the role of $GABA_B$ receptors on the slow oscillatory rhythmicity driven by the alternating between Up and Down states. To that end we combined extracellular recordings of spontaneously active cortical network slices and computational experiments to further understand the mechanisms underlying slow wave activity. We found that $GABA_B$ receptors controlled the duration of the active periods or Up states, such that their blockage elongated them, as previously described (Mann et al., 2009). We found that this effect was not mediated by the control of the firing rate during the Up state, but by contributing to the Up to Down transition, thus controlling the network synchronization. Furthermore, $GABA_B$ receptors also had an impact on the subsequent silent periods or Down states, therefore modulating the complete oscillatory cycle. Interestingly, the effect of $GABA_B$ receptor-blockade on the duration of the Down states can be elongation (most commonly), but also shortening. We explore in our computer model how these two opposing effects can be caused by the same intervention. The regularity of the oscillatory cycle is another parameter of the Up/Down dynamics that is modulated by $GABA_B$ receptors, such that their blockade enhances the regularity and their activation introduces dynamical richness.

Although several biophysical mechanisms explaining SWO have been proposed, a full characterization of each one's effects and a systematic study of their interactions is still missing. The difficulty with such studies is the fact that SWO is a spontaneous activity that emerges from the network and most mechanisms interact and influence globally the network dynamics, therefore the precise dissection of individual mechanisms is not an easy task. For example, a mechanism that only affects the firing rate during Up states, is going to modify not only Up but also Down states, since they are dynamically related. Further, the fact that one mechanism investigated by an external intervention (e.g. an agonist/antagonist) introduces a change in the Up/Down dynamics, does not guarantee the extent of its participation under physiological conditions or its interactions with other mechanisms. It is for this reason that these mechanisms are not yet well known and also why we need the use of computational models alongside the experiments to better explore a larger

parameter space and mechanistic interactions.

The blockade of $GABA_B$ inhibition resulted in this study and in others (Mann et al., 2009; Craig et al., 2013) in a consistent elongation of the Up states. Were $GABA_B$ blockade to result in a decreased firing rate of the network, the Up state elongation could be seen as an indirect effect. However, the absence of effect on the firing rate points to a direct role of $GABA_B$ inhibition in the termination of Up states. We observed that the average elongation (both in typical and atypical cases) of Up states was up to 182%, which in absolute terms is an elongation from an average of 0.56 (control) to 0.93 (after CGP 35348) seconds. Out of 37 cases, only 3 of them did not show an elongation of the Up state duration as a result of $GABA_B$ blockade. All the rest elongated in a range that varied between 111% and 368%. Interestingly, this variability was independent of the original duration of Up states, which varied between 0.21 and 1.31 seconds, suggesting that $GABA_B$ does not have a preferential role in Up state termination for either short or long Up states. Elongation was also independent of firing rate during Up states. This suggests that $GABA_B$ is an independent mechanism that terminates Up states by acting in cooperation with other mechanisms, as it is the case for $GABA_A$ receptors. The blockade of fast inhibition, mediated by $GABA_A$ receptors results in increased firing rates in the Up states, that efficiently activate activity dependent mechanisms, such as potassium currents, that induce the termination of Up states, and shorten them (Sanchez-Vives et al., 2010). The role of $GABA_A$ receptors on the termination of Up states and the initiation of the Down states suggests that they may as well have a role in the so-called Off-periods that disrupt local causal interactions in the cortical network in unresponsive wakefulness syndrome and natural sleep (Rosanova et al., 2018).

The impact of $GABA_B$ inhibition on the variability of intervals also suggests that the participation of $GABA_B$ in the termination of Up states varies depending on the functional state of the network, decreasing for those states that are highly regular. In the experimental study, we found that the regularity of the cycle significantly increased when $GABA_B$ receptors were blocked. In the model, by blocking $GABA_B$ the network went into an oscillatory alternation of states dominated by adaptation mechanisms, resulting in a more regular oscillatory rhythm. This shows that $GABA_B$

activation not only plays a role in the termination of Up states, but also introduces variability in the oscillatory cycle. That the regularity of the oscillatory cycle can range from very high in deep (slow-wave) sleep or anesthesia to very low and chaotic during periods of transition to the awake state (Deco et al., 2009) suggests that different mechanisms regulate transitions between Up and Down states in different functional states. According to our results, a reduced contribution of $GABA_B$ inhibition to the dynamics of the SWO would be expected in highly regular periods of activity such as deep sleep or anesthesia which, according to our model, could be well regulated by adaptation mechanisms. Experiments in awake rodents have shown different degrees of network synchronization: whereas alert states are characterized by desynchronized activity, resting awake states are characterized by more synchronized activity, with slow spontaneous fluctuations (Poulet and Petersen, 2008; Okun et al., 2010). $GABA_B$ receptors could be involved in switching between these different functional states by modulating the network synchronization.

It has been shown that electrical stimulation of layer I is effective in terminating Up states (Mann et al., 2009). This effect is blocked by the $GABA_B$ receptor-blocker CGP55845, suggesting that the Up state termination is mediated by $GABA_B$ activation triggered by a subtype of interneuron in layer 1 called neurogliaform cell (Hestrin and Armstrong, 1996; Olah et al., 2007). However, our experimental results show that the termination of the spontaneous Up states seems to be independent of layer 1-mediated activation. Different roles for $GABA_{B1a}$ and $GABA_{B1b}$ subunits have also been proposed. $GABA_{B1a}$ is preferentially located presynaptically and seems to be involved in spontaneous Up state termination; $GABA_{B1b}$, on the other hand, is related to afferent or electrical stimulation via layer 1 activation (Craig et al., 2013). In our experiments, the disconnection of layer 1 from the slices did not result in the elongation of Up states; instead, Up state duration did not change or in some cases became shorter. However, applying $GABA_B$ blocker CGP 35348 after removing layer 1, Up states increased their duration as it occurred in slices where layer 1 was not removed (Fig. S1). This result is in agreement with previous ones showing that spontaneous Up-to-Down transitions are independent of layer 1 activation (Craig et al., 2013). Craig et al. (2013) suggested that the change in the Up-to-Down transition

slope is mediated by presynaptic $GABA_{B1a}$ receptor activation. In this operational framework, our model predicted that changes in NMDA conductance together with firing rate adaptation are enough to generate activity in two different networks, similar to the ones we observed experimentally after blocking $GABA_B$ receptors, as we showed for the typical and the atypical cases.

We also analyzed the effect of blockage of $GABA_B$ in supragranular layers and the result was similar, showing that the modulation of the activity by $GABA_B$ persisted in different layers and also in different cortical areas, in our case visual and prefrontal, and compatible with other authors' and our own work (Mann et al., 2009; Wang et al., 2010; Craig et al., 2013).

We previously described that the partial blockade of $GABA_A$ receptors with bicuculline increases the firing rate during Up states and decreases their regularity in active ferret cortical slices (Sanchez-Vives et al., 2010). More recently, Busche and colleagues showed, in wild-type anesthetized mice, that small concentrations of gabazine (a $GABA_A$ receptor antagonist) desynchronize the network activity between distal cortical areas, and treatment with benzodiazepine ($GABA_A$ agonist) restored the synchronization in a mouse model of Alzheimer's disease characterized by low levels of synchronization in the control condition (Busche et al., 2015). Here, we show how the blockade of $GABA_B$ receptors increases the regularity of the SWO, suggesting that $GABA_B$ can introduce desynchronization in normal conditions. On this basis, we propose a model in which GABA can modulate the network synchronization by means of the activation of $GABA_A$ and $GABA_B$ receptors which generate opposing effects, synchronizing or desynchronizing the activity, respectively.

Activity-dependent adaptation, mediated by hyperpolarizing currents, has been proposed as a critical mechanism for the termination of Up states and maintenance of Down states. Such currents would be Ca^{2+} and Na^{+}-dependent K^{+} currents (Compte et al., 2003; Sanchez-Vives et al., 2010) or AMPc-dependent potassium currents (Cunningham et al., 2006). Hyperpolarizing currents can also interact with other mechanisms such as synaptic depression, modulating the emerging patterns (Benita et al., 2012). Adaptation has also been considered in the dynamics of Up/Down states

as a necessary mechanism, but in a more ample sense, such that it could include either hyperpolarizing ionic currents but also synaptic inhibition (Mattia and Sanchez-Vives, 2012). Here, in our model we considered firing rate adaptation and $GABA_B$ receptors as the two dominant biophysical factors responsible for the termination of Down states and used experimental and modeling work to investigate how they participate in slow oscillations.

The model is a generalization of the standard leaky integrate-and-fire model in which a nonlinear current has been included (Parga and Abbott, 2007). Adaptation is taken as a linear firing adaptation current with a characteristic time appropriate for generating oscillations with an adequate frequency. A more complete way to describe adaptation in these slices is through an activity-dependent mechanism based on Na^+ and Ca^2-dependent K^+ currents (Compte et al., 2003). In this case, spike firing during Up states induces the accumulation of Na^+ and Ca^{2+} ions inside the axon, which in turn causes K^+ ions to move outside the axon, hence hyperpolarizing the neuron and terminating Up states. The duration of this hyperpolarization is determined by the time course of the decay of the Na^+ and Ca^{2+} concentrations (Wang et al., 2003), giving rise to Down states. However, a modeling framework where a simpler activity-dependent adaptation is responsible for the Up-to-Down state transitions produces, in the absence of $GABA_B$ receptors, oscillations as regular as those observed in the slices. Our model considers firing rate adaptation and slow inhibition by $GABA_B$ as the two biophysical elements determining the SWO; another plausible mechanism is short-term synaptic dynamics (Timofeev et al., 2000; Melamed et al., 2008; Benita et al., 2012); however, we did not need it to explain the slice behavior.

In conclusion, using *in vitro* experiments and computer models, we found that $GABA_B$ receptors critically control the synchronization of the network discharge. According to our results the decrease in $GABA_B$ receptor activation enhances the cycle regularity and Up state duration. This suggests that in normal conditions, $GABA_B$ is a source of desynchronization in cortical activity.

Acknowledgements

This work was supported by EU H2020 Research and Innovation Programme, Grant 785907 (HBP SGA2) and BFU2017-85048-R (MINECO). We would like to thank Tony Donegan for editing the paper.

References

Aghajanian GK, Rasmussen K (1989) Intracellular studies in the facial nucleus illustrating a simple new method for obtaining viable motoneurons in adult rat brain slices. Synapse 3:331–338 Available at: http://www.ncbi.nlm.nih.gov/pubmed/2740992 [Accessed July 26, 2018].

Aserinsky E, Kleitman N (1953) Regularly occurring periods of eye motility, and concomitant phenomena, during sleep. Science 118:273–274 Available at: http://www.ncbi.nlm.nih.gov/pubmed/13089671 [Accessed July 26, 2018].

Benita JM, Guillamon A, Deco G, Sanchez-Vives M V. (2012) Synaptic depression and slow oscillatory activity in a biophysical network model of the cerebral cortex. Front Comput Neurosci 6:64 Available at: http://journal.frontiersin.org/article/10.3389/fncom.2012.00064/abstract [Accessed February 21, 2019].

Bettinardi RG, Tort-Colet N, Ruiz-Mejias M, Sanchez-Vives M V, Deco G (2015) Gradual emergence of spontaneous correlated brain activity during fading of general anesthesia in rats: Evidences from fMRI and local field potentials. Neuroimage 114:185–198.

Bullock TH, McClune MC (1989) Lateral coherence of the electrocorticogram: a new measure of brain synchrony. In: How do Brains Work?, pp 375–396. Birkhäuser Boston. Available at: https://doi.org/10.1007%2F978-1-4684-9427-3_33.

Busche MA, Kekuš M, Adelsberger H, Noda T, Förstl H, Nelken I, Konnerth A (2015) Rescue of long-range circuit dysfunction in Alzheimer's disease models. Nat Neurosci 18:1623–1630 Available at: http://www.nature.com/articles/nn.4137 [Accessed July 26, 2018].

Butz M, Gross J, Timmermann L, Moll M, Freund HJ, Witte OW, Schnitzler A (2004) Perilesional pathological oscillatory activity in the magnetoencephalogram of patients with cortical brain lesions. Neurosci Lett 355:93–96.

Castano-Prat P, Perez-Mendez L, Perez-Zabalza M, Sanfeliu C, Giménez-Llort L, Sanchez-Vives MVMV (2019) Altered slow (<1Hz) and fast (beta and gamma) neocortical oscillations in the 3xTg-AD mouse model of Alzheimer's disease under anesthesia. Neurobiol Aging 79:142–151.

Castano-Prat P, Perez-Zabalza M, Perez-Mendez L, Escorihuela RM, Sanchez-Vives M V (2017) Slow and Fast Neocortical Oscillations in the Senescence-Accelerated Mouse Model SAMP8. Front Aging Neurosci 9:141.

Chatfield C (1980) The analysis of time series : an introduction. London: Chapman & Hall/CRC.

Compte A, Reig R, Sanchez-Vives M V. (2009) Timing Excitation and Inhibition in the Cortical Network. In: Coherent Behavior in Neuronal Networks, pp 17–46. New York, NY: Springer New York. Available at: http://link.springer.com/10.1007/978-1-4419-0389-1_2 [Accessed July 18, 2019].

Compte A, Sanchez-Vives M V, McCormick DA, Wang X-J (2003) Cellular and network mechanisms of slow oscillatory activity (. J Neurophysiol 89:2707–2725 Available at: http://www.physiology.org/doi/10.1152/jn.00845.2002 [Accessed July 26, 2018].

Craig MT, Mayne EW, Bettler B, Paulsen O, McBain CJ (2013) Distinct roles of {GABAB}1a- and {GABAB}1b-containing {GABABreceptors} in spontaneous and evoked termination of persistent cortical activity. J Physiol 591:835–843 Available at: https://doi.org/10.1113%2Fjphysiol.2012.248088.

Cunningham MO, Pervouchine DD, Racca C, Kopell NJ, Davies CH, Jones RSG, Traub RD, Whittington MA (2006) Neuronal metabolism governs cortical network response state. Proc Natl Acad Sci 103:5597–5601 Available at: https://doi.org/10.1073%2Fpnas.0600604103.

Dasilva M, Navarro-Guzman A, Ortiz-Romero P, Camassa A, Muñoz-Cespedes A,

Campuzano V, Sanchez-Vives M V. (2019) Altered Neocortical Dynamics in a Mouse Model of Williams–Beuren Syndrome. Mol Neurobiol.

Deco G, Martí D, Ledberg A, Reig R, Sanchez Vives M V (2009) Effective reduced diffusion-models: a data driven approach to the analysis of neuronal dynamics. Friston KJ, ed. PLoS Comput Biol 5:e1000587 Available at: http://dx.plos.org/10.1371/journal.pcbi.1000587 [Accessed July 26, 2018].

Destexhe A, Contreras D, Steriade M (1999) Spatiotemporal analysis of local field potentials and unit discharges in cat cerebral cortex during natural wake and sleep states. J Neurosci 19:4595–4608 Available at: http://www.ncbi.nlm.nih.gov/pubmed/10341257 [Accessed July 18, 2019].

Diekelmann S, Born J (2010) The memory function of sleep. Nat Rev Neurosci 11:114–126 Available at: http://www.nature.com/articles/nrn2762 [Accessed July 26, 2018].

Doesburg SM, Herdman AT, Ribary U, Cheung T, Moiseev A, Weinberg H, Liotti M, Weeks D, Grunau RE (2010) Long-range synchronization and local desynchronization of alpha oscillations during visual short-term memory retention in children. Exp brain Res 201:719–727 Available at: http://link.springer.com/10.1007/s00221-009-2086-9 [Accessed July 26, 2018].

Dowse HB (2009) Chapter 6 Analyses for Physiological and Behavioral Rhythmicity. In: Methods in Enzymology, pp 141–174. Elsevier. Available at: http://linkinghub.elsevier.com/retrieve/pii/S0076687908038068 [Accessed July 26, 2018].

Gloor P, Ball G, Schaul N (1977) Brain lesions that produce delta waves in the EEG. Neurology 27:326–333.

Harris KD, Thiele A (2011) Cortical state and attention. Nat Rev Neurosci 12:509–523.

Hestrin S, Armstrong WE (1996) Morphology and physiology of cortical neurons in

layer I. J Neurosci 16:5290–5300 Available at: http://www.ncbi.nlm.nih.gov/pubmed/8757242 [Accessed July 18, 2019].

Hoffman KL, Battaglia FP, Harris K, MacLean JN, Marshall L, Mehta MR (2007) The upshot of up states in the neocortex: from slow oscillations to memory formation. J Neurosci 27:11838–11841 Available at: http://www.ncbi.nlm.nih.gov/pubmed/17978020 [Accessed July 26, 2018].

Klimesch W, Sauseng P, Hanslmayr S (2007) EEG alpha oscillations: the inhibition-timing hypothesis. Brain Res Rev 53:63–88 Available at: http://www.ncbi.nlm.nih.gov/pubmed/16887192 [Accessed July 26, 2018].

Little S, Brown P (2014) The functional role of beta oscillations in Parkinson's disease. Parkinsonism Relat Disord 20 Suppl 1:S44-8 Available at: http://linkinghub.elsevier.com/retrieve/pii/S1353802013700130 [Accessed July 26, 2018].

Luczak A, Barthó P, Marguet SL, Buzsáki G, Harris KD (2007) Sequential structure of neocortical spontaneous activity in vivo. Proc Natl Acad Sci U S A 104:347–352 Available at: https://doi.org/10.1073%2Fpnas.0605643104 [Accessed July 26, 2018].

Mann EO, Kohl MM, Paulsen O (2009) Distinct roles of GABA(A) and GABA(B) receptors in balancing and terminating persistent cortical activity. J Neurosci 29:7513–7518 Available at: http://www.jneurosci.org/cgi/doi/10.1523/JNEUROSCI.6162-08.2009 [Accessed July 26, 2018].

Mattia M, Sanchez-Vives M V. (2012) Exploring the spectrum of dynamical regimes and timescales in spontaneous cortical activity. Cogn Neurodyn 6:239–250 Available at: http://www.ncbi.nlm.nih.gov/pubmed/23730355 [Accessed July 18, 2019].

Melamed O, Barak O, Silberberg G, Markram H, Tsodyks M (2008) Slow oscillations

in neural networks with facilitating synapses. J Comput Neurosci 25:308–316 Available at: http://link.springer.com/10.1007/s10827-008-0080-z [Accessed July 26, 2018].

Okun M, Lampl I (2008) Instantaneous correlation of excitation and inhibition during ongoing and sensory-evoked activities. Nat Neurosci 11:535–537 Available at: http://www.nature.com/articles/nn.2105 [Accessed July 26, 2018].

Okun M, Naim A, Lampl I (2010) The subthreshold relation between cortical local field potential and neuronal firing unveiled by intracellular recordings in awake rats. J Neurosci 30:4440–4448 Available at: http://www.ncbi.nlm.nih.gov/pubmed/20335480 [Accessed July 18, 2019].

Olah S, Komlosi G, Szabadics J, Varga C, Toth E, Barzo P, Tamas G (2007) Output of neurogliaform cells to various neuron types in the human and rat cerebral cortex. Front Neural Circuits 1:4.

Parga N, Abbott LF (2007) Network model of spontaneous activity exhibiting synchronous transitions between up and down States. Front Neurosci 1:57–66 Available at: http://journal.frontiersin.org/article/10.3389/neuro.01.1.1.004.2007/abstract [Accessed July 26, 2018].

Poulet JFA, Petersen CCH (2008) Internal brain state regulates membrane potential synchrony in barrel cortex of behaving mice. Nature 454:881–885 Available at: http://www.nature.com/articles/nature07150 [Accessed July 26, 2018].

Reig R, Mattia M, Compte A, Belmonte C, Sanchez-Vives M V. (2010) Temperature Modulation of Slow and Fast Cortical Rhythms. J Neurophysiol 103:1253–1261 Available at: http://www.physiology.org/doi/10.1152/jn.00890.2009 [Accessed July 26, 2018].

Renart A, de la Rocha J, Bartho P, Hollender L, Parga N, Reyes A, Harris KD (2010) The asynchronous state in cortical circuits. Science 327:587–590 Available at:

http://www.sciencemag.org/cgi/doi/10.1126/science.1179850 [Accessed July 26, 2018].

Rosanova M, Fecchio M, Casarotto S, Sarasso S, Casali AG, Pigorini A, Comanducci A, Seregni F, Devalle G, Citerio G, Bodart O, Boly M, Gosseries O, Laureys S, Massimini M (2018) Sleep-like cortical OFF-periods disrupt causality and complexity in the brain of unresponsive wakefulness syndrome patients. Nat Commun 9:4427 Available at: http://www.nature.com/articles/s41467-018-06871-1 [Accessed August 28, 2019].

Rubenstein JLR, Merzenich MM (2003) Model of autism: Increased ratio of excitation/inhibition in key neural systems. Genes, Brain Behav 2:255–267.

Ruiz-Mejias M, Ciria-Suarez L, Mattia M, Sanchez-Vives M V. (2011) Slow and fast rhythms generated in the cerebral cortex of the anesthetized mouse. J Neurophysiol 106:2910–2921.

Ruiz-Mejias M, Martinez de Lagran M, Mattia M, Castano-Prat P, Perez-Mendez L, Ciria-Suarez L, Gener T, Sancristobal B, García-Ojalvo J, Gruart A, Delgado-García JM, Sanchez-Vives M V, Dierssen M (2016) Overexpression of Dyrk1A, a Down Syndrome Candidate, Decreases Excitability and Impairs Gamma Oscillations in the Prefrontal Cortex. J Neurosci 36:3648–3659.

Sanchez-Vives M V., Massimini M, Mattia M (2017) Shaping the Default Activity Pattern of the Cortical Network. Neuron 94:993–1001.

Sanchez-Vives M V., Mattia M (2014) Slow wave activity as the default mode of the cerebral cortex. Arch Ital Biol 152:2–3 Available at: http://www.ncbi.nlm.nih.gov/pubmed/25828686 [Accessed August 26, 2019].

Sanchez-Vives M V., McCormick DA (2000) Cellular and network mechanisms of rhythmic recurrent activity in neocortex. Nat Neurosci 3:1027–1034 Available at: http://www.ncbi.nlm.nih.gov/pubmed/11017176 [Accessed August 26, 2019].

Sanchez-Vives M V, Mattia M, Compte A, Perez-Zabalza M, Winograd M, Descalzo

VF, Reig R (2010) Inhibitory modulation of cortical up states. J Neurophysiol 104:1314–1324 Available at: http://www.ncbi.nlm.nih.gov/pubmed/20554835 [Accessed October 31, 2018].

Shu Y, Hasenstaub A, McCormick DA (2003) Turning on and off recurrent balanced cortical activity. Nature 423:288–293.

Stancák A, Pfurtscheller G (1996) Event-related desynchronisation of central beta-rhythms during brisk and slow self-paced finger movements of dominant and nondominant hand. Brain Res Cogn Brain Res 4:171–183 Available at: http://www.ncbi.nlm.nih.gov/pubmed/8924046 [Accessed July 26, 2018].

Steriade M, Nuñez A, Amzica F (1993) A novel slow (< 1 Hz) oscillation of neocortical neurons in vivo: depolarizing and hyperpolarizing components. J Neurosci 13:3252–3265 Available at: http://www.ncbi.nlm.nih.gov/pubmed/8340806 [Accessed July 18, 2019].

Timofeev I, Grenier F, Bazhenov M, Sejnowski TJ, Steriade M (2000) Origin of slow cortical oscillations in deafferented cortical slabs. Cereb Cortex 10:1185–1199 Available at: http://www.ncbi.nlm.nih.gov/pubmed/11073868 [Accessed July 26, 2018].

Tononi G, Cirelli C (2014) Sleep and the price of plasticity: from synaptic and cellular homeostasis to memory consolidation and integration. Neuron 81:12–34 Available at: http://linkinghub.elsevier.com/retrieve/pii/S0896627313011860 [Accessed July 26, 2018].

Varela F, Lachaux JP, Rodriguez E, Martinerie J (2001) The brainweb: phase synchronization and large-scale integration. Nat Rev Neurosci 2:229–239 Available at: http://www.nature.com/articles/35067550 [Accessed July 26, 2018].

Wang X-J, Liu Y, Sanchez-Vives M V, McCormick DA (2003) Adaptation and temporal decorrelation by single neurons in the primary visual cortex. J

Neurophysiol 89:3279–3293 Available at: http://www.physiology.org/doi/10.1152/jn.00242.2003 [Accessed July 26, 2018].

Wang Y, Neubauer FB, Lüscher H-R, Thurley K (2010) {GABAB} receptor-dependent modulation of network activity in the rat prefrontal cortex in vitro. Eur J Neurosci:no--no Available at: https://doi.org/10.1111%2Fj.1460-9568.2010.07191.x.

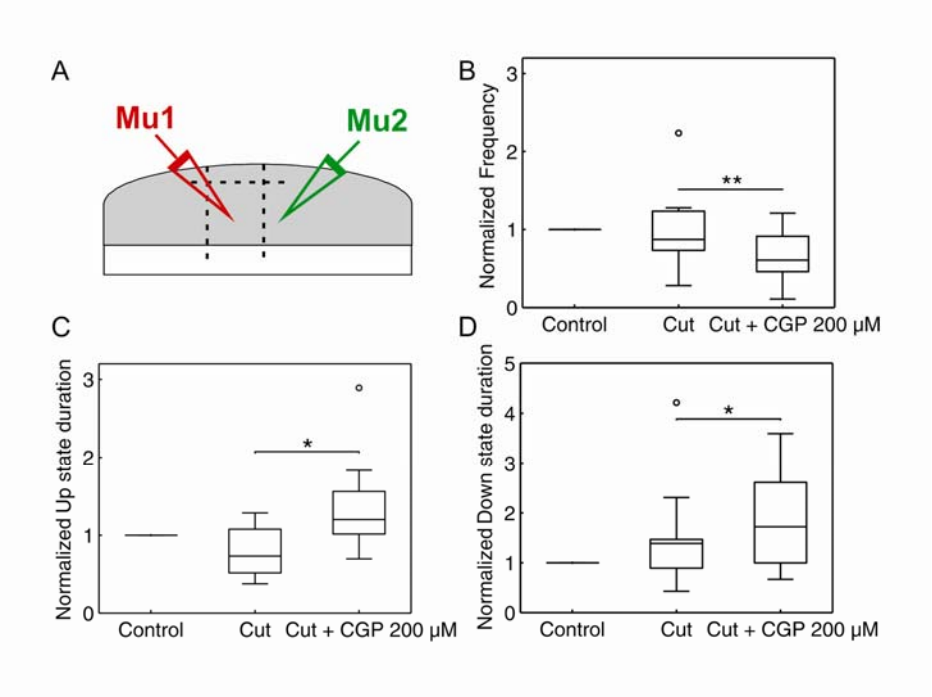

Figure S1. Effects of elimination of layer 1. A. Experimental sketch with double extracellular recordings. B–D. Average of normalized frequency (B), Up state duration (C), and Down state duration (D) in control, after layer 1 cut, and after application of CGP 200μM. A Student's *t*-test was used to evaluate how different the normalized averages were from 1.0., $p < 0.05$ (*); $p < 0.01$ (**); $p < 0.001$ (***). (n= 13).